Progress In Electromagnetics Research, PIER 97, 259–274, 2009

SOLUTION TO ELECTROMAGNETIC SCATTERING BY BI-ISOTROPIC MEDIA USING MULTILEVEL GREEN'S FUNCTION INTERPOLATION METHOD

Y. Shi

School of Electronic Engineering
Xidian University
Xi'an, China

C. H. Chan

State Key Laboratory of Millimeter Waves
City University of Hong Kong
Hong Kong SAR, China

Abstract—In this paper, a multilevel Green's function interpolation method (MLGFIM) is developed to analyze electromagnetic scattering from an arbitrarily shaped three-dimensional objects comprised of both conductor and bi-isotropic media. The field decomposition method is adopted to split the homogeneous bi-isotropic media into two uncoupled isotropic media instead of direct calculation of complicated Green's function in bi-isotropic material. The problem is formulated using the Paggio-Miller-Chang-Harrington-Wu-Tsai (PMCHWT) approach for multiple homogeneous isotropic media and electric field approach for conducting bodies. The resultant integral equations are discretized by the method of moment (MoM) and iteratively solved by MLGFIM. Numerical examples illustrate accuracy of this algorithm and CPU time of $O(N \log N)$ and memory requirement of $O(N)$.

1. INTRODUCTION

Recent developments in material technology have allowed for greater design flexibility and novel application in antennas and microwave components. Specifically, bi-isotropic (BI) materials [1] have emerged as one of the most promising topics in electromagnetic research. Many

Corresponding author: C. H. Chan (eechic@cityu.edu.hk).

possible applications were proposed for radar absorbing materials, waveguide mode converters, and polarization rotators, etc. [2]. Due to the special form of their constitutive relationships, there has been increasing interest in recent years for accurate and efficient analysis of electromagnetic wave propagation and scattering in those materials in microwave range. Using the eigenfunction method [3, 4], analytical solutions are available for some simple geometries such as spheres and cylinders. On the other hand, many efforts have been put into the development of efficient numerical techniques based on either integral or differential equations. The method of moments (MoM) [5, 6], the finite difference time domain (FDTD) approach [7, 8] and T-matrix method [9], etc., have been developed to solve EM scattering by complex bodies consisting of the bi-isotropic media. When the BI objects are homogeneous or piecewise homogeneous, MoM is preferred because it limits the discretization of the unknown quantities to the surfaces of the objects and the discontinuous interfaces between different materials [10–13]. Despite this, the computational requirements for MoM solution of this type of problems are still very high. In this paper, the multilevel Green's function interpolation method (MLGFIM) [14–17] is developed to deal with this problem.

MLGFIM is a recent-developed kernel-independent approach, originally proposed to rapidly solve electro-quasi-static problems [14], and later extended to solve three-dimensional full-wave electromagnetic scattering and radiation problems [15–17]. It inherits the tree structure of the kernel-dependent multilevel fast multipole algorithm (MLFMA) [18–23] and combines interpolation ideas of precorrected fast Fourier transform (PFFT) [24–26]. The peer-level and lower-to-upper level interpolation techniques [14, 15] distinguish MLGFIM from Brandt's method in which a soften kernel is required. The adaptive phase compensation (APC) technique [16] and the hybrid quasi-2D/3D multilevel partitioning approach [17] are proposed in order to improve the interpolation efficiency. To date, MLGFIM has been applied to perfect electric conducting (PEC) objects, coplanar objects and composite objects consisting of conductor and isotropic media in which computational complexities are between $O(N)$ and $O(N \log N)$, and all of memory complexities are $O(N)$.

In this paper, we apply MLGFIM for computing electromagnetic scattering from 3D bodies comprising both conducting and BI media objects. The field decomposition approach [1] is employed to split the homogeneous BI medium into two uncoupled isotropic media. We formulate the surface integral equations (SIE) using the Paggio-Miller-Chang-Harrington-Wu-Tsai (PMCHWT) approach [27, 28] for multiple homogeneous isotropic media and the electric field approach

for conducting objects. The resultant integral equations are discretized by MoM. MLGFIM is then used to speed up the matrix-vector multiplication in the iterative solution process. Numerical examples demonstrate the good performance of the proposed approach.

2. FORMULATIONS

2.1. Surface Integral Equation

Consider an arbitrary structure comprised of multiple conducting and dielectric objects, as shown in Fig. 1. The j-th dielectric object is the homogeneous bi-isotropic medium, of which the constitutive relationships can be expressed as

$$\vec{D} = \varepsilon\vec{E} + \xi\vec{H} \tag{1}$$

$$\vec{B} = \zeta\vec{E} + \mu\vec{H} \tag{2}$$

in which

$$\xi = (\chi + i\kappa)\sqrt{\mu_0\varepsilon_0} \tag{3}$$

$$\zeta = (\chi - i\kappa)\sqrt{\mu_0\varepsilon_0} \tag{4}$$

The BI medium with $\kappa = 0$ but $\chi \neq 0$ is called the Tellegen medium, while the one with $\chi = 0$ but $\kappa \neq 0$ is called the Pasteur medium or Chiral medium.

Let us denote the homogeneous exterior region as region 0 and other homogeneous dielectric region as region i ($i = 1, 2, \ldots$). The surface of region i is denoted as S_i and the interface between regions i and j is denoted as S_{ij}. The unit normal to S_{ij} and pointing toward the interior of region i is denoted as $\hat{n}_{ij}$. Hence we have $\hat{n}_{ij} = -\hat{n}_{ji}$.

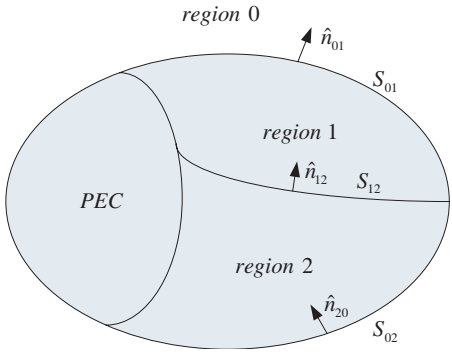

Figure 1. Composite metallic and dielectric scatterer.

In each region consisting of bi-isotropic medium, for instance region j, electric field $\vec{E}$, magnetic field $\vec{H}$, electric current $\vec{J}$ and magnetic current $\vec{M}$ can be split into two uncoupled electromagnetic quantities as follows:

$$\vec{E}_j = \vec{E}_j^{+} + \vec{E}_j^{-} \tag{5}$$

$$\vec{H}_j = \vec{H}_j^{+} + \vec{H}_j^{-} \tag{6}$$

$$\vec{J}_j = \vec{J}_j^{+} + \vec{J}_j^{-} \tag{7}$$

$$\vec{M}_j = \vec{M}_j^{+} + \vec{M}_j^{-} \tag{8}$$

where

$$\vec{E}_j^{\pm} = \frac{1}{2\cos\vartheta}\left(e^{\pm i\vartheta}\vec{E}_j \pm i\eta\vec{H}_j\right) \tag{9}$$

$$\vec{H}_j^{\pm} = \frac{1}{2\cos\vartheta}\left(e^{\mp i\vartheta}\vec{H}_j \mp \frac{i}{\eta}\vec{E}_j\right) \tag{10}$$

$$\vec{J}_j^{\pm} = \frac{1}{2\cos\vartheta}\left(e^{\mp i\vartheta}\vec{J}_j \pm \frac{i}{\eta}\vec{M}_j\right) \tag{11}$$

$$\vec{M}_j^{\pm} = \frac{1}{2\cos\vartheta}\left(e^{\pm i\vartheta}\vec{M}_j \mp i\eta\vec{J}_j\right) \tag{12}$$

$$\vartheta = \sin^{-1}\frac{\chi}{n} \tag{13}$$

$$n = \sqrt{(\mu_j\varepsilon_j)/(\mu_0\varepsilon_0)} \tag{14}$$

and $\eta = \sqrt{\mu_j/\varepsilon_j}$ is the intrinsic impedance.

Two uncoupled electromagnetic quantities satisfy Maxwell's equations in homogeneous isotropic medium, i.e.,

$$\nabla\times\vec{E}_j^{\pm} = i\omega\mu_j^{\pm}\vec{H}_j^{\pm} - \vec{M}_j^{\pm} \tag{15}$$

$$\nabla\times\vec{H}_j^{\pm} = -i\omega\varepsilon_j^{\pm}\vec{E}_j^{\pm} + \vec{J}_j^{\pm} \tag{16}$$

in which

$$\varepsilon_j^{\pm} = \varepsilon\left(\cos\vartheta \pm \frac{\kappa}{n}\right)e^{\mp i\vartheta} \tag{17}$$

$$\mu_j^{\pm} = \mu\left(\cos\vartheta \pm \frac{\kappa}{n}\right)e^{\pm i\vartheta} \tag{18}$$

In this scenario, the electric field integral equation (EFIE) and

magnetic field integral equation (MFIE) can be obtained as

$$\sum_{\pm}\left[\sum_{m}-\frac{1}{i\omega\varepsilon_j^{\pm}}L_j\left(\vec{J}_{jm}^{\pm}\right)-K_j\left(\vec{M}_{jm}^{\pm}\right)\right]_{\tan}=-\vec{E}_j^{inc}\Big|_{\tan} \quad (19)$$

$$\sum_{\pm}\left[\sum_{m}K_j\left(\vec{J}_{jm}^{\pm}\right)-\frac{1}{i\omega\mu_j^{\pm}}L_j\left(\vec{M}_{jm}^{\pm}\right)\right]_{\tan}=-\vec{H}_j^{inc}\Big|_{\tan} \quad (20)$$

where

$$\begin{aligned}L_j\left(\vec{X}_{jm}^{\pm}\right) &= \frac{\left(k_j^{\pm}\right)^2}{4\pi}\int\limits_{S_{jm}}G_j^{\pm}\left(\vec{r},\vec{r}\,'\right)\vec{X}_{jm}^{\pm}\left(\vec{r}\,'\right)ds'\\ &\quad+\frac{1}{4\pi}\int\limits_{S_{jm}}\nabla G_j^{\pm}\left(\vec{r},\vec{r}\,'\right)\nabla_s'\cdot\vec{X}_{jm}^{\pm}\left(\vec{r}\,'\right)ds' \quad (21)\\ K_j\left(\vec{X}_{jm}^{\pm}\right) &= \frac{1}{4\pi}\int\limits_{S_{jm}}\nabla G_j^{\pm}\left(\vec{r},\vec{r}\,'\right)\times\vec{X}_{jm}^{\pm}\left(\vec{r}\,'\right)ds'\\ &\quad+\frac{1}{2}\hat{n}_{jm}\times\vec{X}_{jm}^{\pm}\left(\vec{r}\right) \quad (22)\\ G_j^{\pm}\left(\vec{r},\vec{r}\,'\right) &= \frac{e^{ik_j^{\pm}\left|\vec{r}-\vec{r}\,'\right|}}{\left|\vec{r}-\vec{r}\,'\right|} \quad (23)\\ k_j^{\pm} &= \omega\sqrt{\varepsilon_j^{\pm}\mu_j^{\pm}} \quad (24)\end{aligned}$$

Furthermore, equivalent electric current $\vec{J}_{jm}^{\pm}$ and equivalent magnetic current $\vec{M}_{jm}^{\pm}$ are defined by

$$\vec{J}_{jm}^{\pm}=\hat{n}_{jm}\times\vec{H}^{\pm}\left(\vec{r}\right)\quad\vec{r}\in S_{jm} \quad (25)$$

$$\vec{M}_{jm}^{\pm}=-\hat{n}_{jm}\times\vec{E}^{\pm}\left(\vec{r}\right)\quad\vec{r}\in S_{jm} \quad (26)$$

The EFIE and MFIE in region j are (19) and (20) carried over all the interfaces which surround region j. Using PMCHWT approach, we can combine EFIE and MFIE on the interface between two dielectric

regions to obtain integral equations on $S_{jj'}$ as follows:

$$\begin{aligned}
&\sum_{\pm}\left[\sum_{m}-\frac{1}{i\omega\varepsilon_j^{\pm}}L_j\left(\vec{J}_{jm}^{\pm}\right)-K_j\left(\vec{M}_{jm}^{\pm}\right)\right]_{\tan}\\
&-\sum_{\pm}\left[\sum_{m'}-\frac{1}{i\omega\varepsilon_{j'}^{\pm}}L_{j'}\left(\vec{J}_{j'm'}^{\pm}\right)-K_{j'}\left(\vec{M}_{j'm'}^{\pm}\right)\right]_{\tan}\\
=\;&-\vec{E}_j^{inc}\Big|_{\tan}+\vec{E}_{j'}^{inc}\Big|_{\tan} \qquad (27)\\
&\sum_{\pm}\left[\sum_{m}K_j\left(\vec{J}_{jm}^{\pm}\right)-\frac{1}{i\omega\mu_j^{\pm}}L_j\left(\vec{M}_{jm}^{\pm}\right)\right]_{\tan}\\
&-\sum_{\pm}\left[\sum_{m'}K_{j'}\left(\vec{J}_{j'm'}^{\pm}\right)-\frac{1}{i\omega\mu_{j'}^{\pm}}L_{j'}\left(\vec{M}_{j'm'}^{\pm}\right)\right]_{\tan}\\
=\;&-\vec{H}_j^{inc}\Big|_{\tan}+\vec{H}_{j'}^{inc}\Big|_{\tan} \qquad (28)
\end{aligned}$$

In addition, since the tangential electric field vanishes on the surface of perfect conductor, only EFIE (19) will be needed.

2.2. Multilevel Green's Function Interpolation Method

The integral equations can be numerically solved using the method of moments (MoM). By applying MoM, the surface is meshed into a number of the curvilinear quadrilateral patches. The unknown electric and magnetic currents are expanded using the zeroth divergence conforming basis (DCB) function [29] (i.e., rooftop basis function) as follows:

$$\vec{J}=\sum_n J_n\vec{f}_n \qquad (29)$$

$$\vec{M}=\sum_n M_n\vec{f}_n \qquad (30)$$

Substituting (11), (12), (29) and (30) into (27) and (28) and applying Galerkin method, we have corresponding matrix equation as

$$\begin{bmatrix} Z^{EJ} & Z^{EM} \\ Z^{HJ} & Z^{HM} \end{bmatrix}\begin{bmatrix} J \\ M \end{bmatrix}=\begin{bmatrix} V^E \\ V^H \end{bmatrix} \qquad (31)$$

where

$$Z_{uv}^{EJ}=\sum_j\left\langle\vec{f}_u,\sum_{\pm}\left[-\frac{1}{i\omega\varepsilon_j^{\pm}}\frac{e^{\mp i\vartheta}}{2\cos\vartheta}L_j\vec{f}_v\pm\frac{i\eta}{2\cos\vartheta}K_j\vec{f}_v\right]\right\rangle \qquad (32)$$

$$Z_{uv}^{EM} = \sum_j \left\langle \vec{f}_u, \sum_{\pm} \left[-\frac{1}{i\omega\varepsilon_j^{\pm}} \frac{e^{\pm i\vartheta}}{2\cos\vartheta} L_j \vec{f}_v \mp \frac{i}{2\eta\cos\vartheta} K_j \vec{f}_v \right] \right\rangle \quad (33)$$

$$Z_{uv}^{HJ} = \sum_j \left\langle \vec{f}_u, \sum_{\pm} \left[\frac{e^{\mp i\vartheta}}{2\cos\vartheta} K_j \vec{f}_v \pm \frac{1}{i\omega\mu_j^{\pm}} \frac{i\eta}{2\cos\vartheta} L_j \vec{f}_v \right] \right\rangle \quad (34)$$

$$Z_{uv}^{HM} = \sum_j \left\langle \vec{f}_u, \sum_{\pm} \left[\pm \frac{i}{2\eta\cos\vartheta} K_j \vec{f}_v - \frac{1}{i\omega\mu_j^{\pm}} \frac{e^{\pm i\vartheta}}{2\cos\vartheta} L_j \vec{f}_v \right] \right\rangle \quad (35)$$

$$V_u^E = \sum_j \left\langle \vec{f}_u, -\vec{E}_j^{inc} \right\rangle \quad (36)$$

$$V_u^H = \sum_j \left\langle \vec{f}_u, -\vec{H}_j^{inc} \right\rangle \quad (37)$$

In order to reduce the calculation time and memory requirement, MLGFIM is utilized to iteratively solve the matrix equation (31). As mentioned earlier, MLGFM uses an octary-cube-tree multilevel partitioning scheme. Specifically, we first enclose the entire object in a large cube, and then partition the large cube into eight smaller cubes. Each subcube is recursively subdivided into smaller cubes until the finest cubes satisfy the termination criterion. For two elements in same or adjacent finest cubes, their interaction is directly calculated. However, the interaction between two elements in different cubes not immediately adjacent to each other is approximately calculated using Green's function interpolation method. For a problem involving multiple regions, the Green's function interpolation has to be independently performed in each region, while the same tree structure for all regions will be kept.

By observing (32)–(35), we can find that there are two kinds of integrals in matrix elements as follows:

$$I_{uv}^{1j} = \left\langle \vec{f}_u, L_j \vec{f}_v \right\rangle \quad (38)$$

$$I_{uv}^{2j} = \left\langle \vec{f}_u, K_j \vec{f}_v \right\rangle \quad (39)$$

Expanding (38) and (39) into the scalar expression [17], we can get a general form, i.e.,

$$I_{uv}^{j} = \int\limits_{S_u^j} ds \int\limits_{S_v^j} ds' \xi\left(\vec{r}\right) \eta\left(\vec{r}'\right) \Lambda^{(j)}\left(\vec{r}, \vec{r}'\right) \quad (40)$$

For non-adjacent groups, we choose a suitable interpolation function

to approximate $\Lambda^{(j)}(\vec{r}, \vec{r}')$ as [17]

$$\Lambda^{(j)}\left(\vec{r}, \vec{r}'\right) = \sum_{p=1}^{K}\sum_{q=1}^{K} w_u^p(\vec{r}) w_v^q\left(\vec{r}'\right)\Lambda^{(j)}\left(\vec{r}_{u,p}, \vec{r}'_{v,q}\right) \tag{41}$$

in which w_u^p and w_v^q are the pth and qth interpolation functions in field group u and source group v, respectively, and K is the number of interpolation points in both groups. Here $\vec{r}_{u,p}(p = 1, \ldots, K)$ and $\vec{r}'_{v,q}(q = 1, \ldots, K)$ are the interpolation point in field group u and source group v, respectively. Substituting (41) into (40), we can obtain

$$\begin{aligned} I_{uv}^j &= \left[\int_{S_u^j} ds\xi\left(\vec{r}\right)\overline{w}_u^T\left(\vec{r}\right)\right]\overline{\overline{\Lambda}}^{(j)}\left[\int_{S_v^j} ds'\eta\left(\vec{r}'\right)\overline{w}_v\left(\vec{r}'\right)\right] \\ &= \overline{\nu}_u^{T(j)}\cdot\overline{\overline{\Lambda}}^{(j)}\cdot\overline{\mu}_v^{(j)} \end{aligned} \tag{42}$$

where interpolation function matrix $\overline{w}_v\left(\vec{r}'\right)$ can be expressed as $\overline{w}_v\left(\vec{r}'\right) = \left[\begin{array}{ccc} w_v^1\left(\vec{r}'\right) & \ldots & w_v^K\left(\vec{r}'\right)\end{array}\right]^T$, and Green's function matrix $\overline{\overline{\Lambda}}^{(j)}$ can be written as follows:

$$\overline{\overline{\Lambda}}^{(j)} = \left[\begin{array}{ccc} \Lambda^{(j)}\left(\vec{r}_{u1}, \vec{r}'_{v1}\right) & \ldots & \Lambda^{(j)}\left(\vec{r}_{u1}, \vec{r}'_{vK}\right) \\ \vdots & \ddots & \vdots \\ \Lambda^{(j)}\left(\vec{r}_{uK}, \vec{r}'_{v1}\right) & \ldots & \Lambda^{(j)}\left(\vec{r}_{uK}, \vec{r}'_{vK}\right)\end{array}\right] \tag{43}$$

MLGFIM utilizes three procedures, e.g., upward pass (aggregation), translation and downward pass (disaggregation) and two types of interpolation schemes, i.e., the peer-level and lower-to-upper level interpolation techniques to calculate the direct interaction component between two basis function in non-adjacent groups. Detailed procedure about MLGFIM may be referred to [14–17].

3. NUMERICAL RESULTS

In this section, we present some numerical examples to demonstrate the accuracy, efficiency and versatility of the proposed method. All calculations are performed on a computer with 3.0 GHz processor and 3.5 GB RAM. Here the QR factorization technique [30, 31] is used to compress the Green's function matrix with low rank and the GMRES [32, 33] iteration method with a relative error norm of 0.001 is adopted for all simulations.

As the first example, we consider a plane wave scattering from a bi-isotropic sphere with electrical size of $k_0 a = 1.5$ where k_0 is the free space wavenumber and a is the radius of the sphere. The relative permittivity and permeability are $4/(1-\kappa_r^2)$ and $1/(1-\kappa_r^2)$, respectively. Here we choose $\kappa_r = \kappa/\sqrt{\varepsilon_r \mu_r}$ and $\chi = 0$. A θ-polarized plane wave is incident from the direction of $\theta = 180^\circ$ on the sphere and the bistatic RCS is calculated as shown in Fig. 2(a). The result is in very good agreement with results in [5]. Based on these results, we further calculate plane wave scattering from the 3 by 3 sphere array. The distance between the centers of two adjacent spheres is $2.5a$. The co-polarized bistatic radar cross section $\sigma_{\theta\theta}$ and the cross-polarized bistatic radar cross section $\sigma_{\theta\phi}$ are calculated, as shown in Figs. 2(b) and (c). It can be seen from Figs. 2(b) and (c) that co-polarized bistatic RCS decreases and cross-polarized bistatic RCS increases due to inclusion of κ_r.

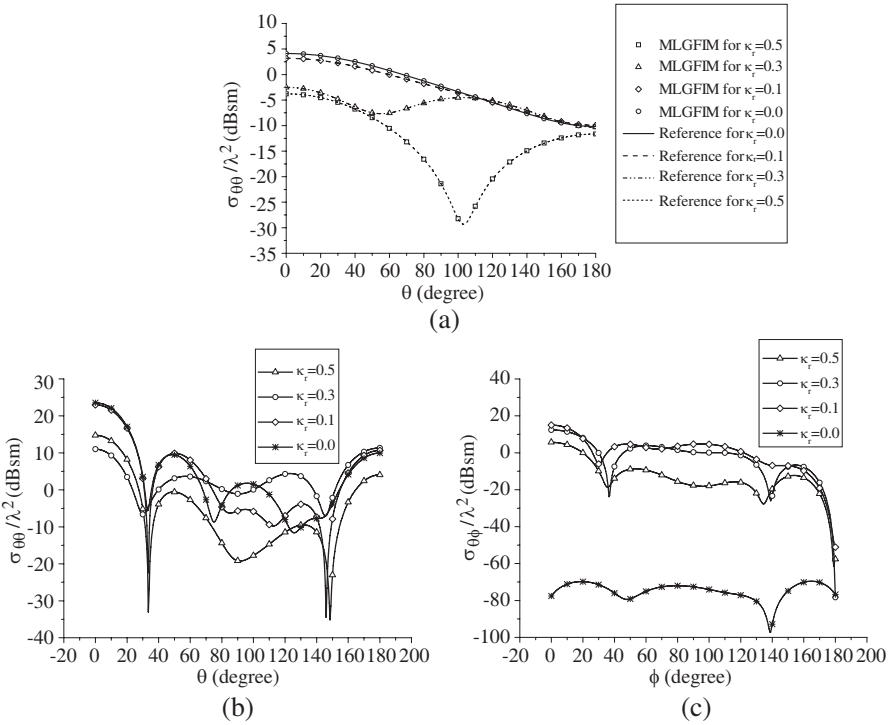

Figure 2. Plane wave scattering from a sphere and a 3-by-3 array of spheres: (a) bistatic RCS with $\theta\theta$ polarization for a single sphere; (b) bistatic RCS with $\theta\theta$ polarization for an array of spheres; (c) bistatic RCS with $\theta\phi$ polarization for an an array of spheres.

In the second case, we consider a plane wave scattering from a three-layer bi-isotropic coated conducting sphere. The radius of conducting sphere is 0.3 m and the radii of three-layer bi-isotropic coated media are 0.45 m, 0.6 m and 0.75 m, respectively. The parameters for three-layer bi-isotropy are $\varepsilon_r = 4$, $\mu_r = 1$, $\kappa_r = 0$, $\chi_r = 0$; $\varepsilon_r = 4.4$, $\mu_r = 1.1$, $\kappa_r = 0.3$, $\chi_r = 0.3$; $\varepsilon_r = 5.3$, $\mu_r = 1.3$, $\kappa_r = 0.5$, $\chi_r = 0.5$, respectively. The co-polarized and cross-polarized bistatic RCS for normally incident plane wave with frequency 300 MHz are calculated. For comparison, two other cases for bi-isotropy with $\chi_r = 0$ and $\kappa_r = 0$ are also calculated, as shown in Figs. 3(a) and (b).

In the following, MLGFIM is applied to plane wave scattering from a 3-by-3 patch array with the finite substrate and ground plane. The geometry of the array can be found in [34], in which

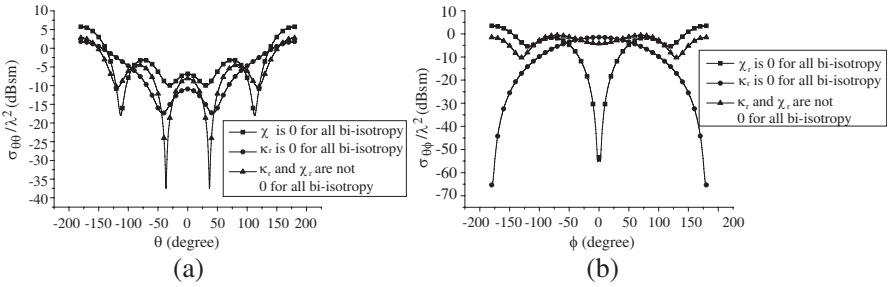

Figure 3. Plane wave scattering from three-layer bi-isotropic coated conducting sphere: (a) bistatic RCS with $\theta\theta$ polarization; (b) bistatic RCS with $\theta\phi$ polarization.

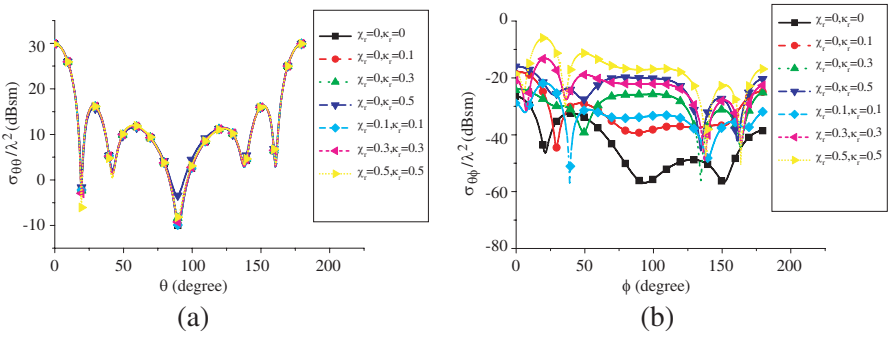

Figure 4. Plane wave scattering from a 3-by-3 array of patch: (a) bistatic RCS with $\theta\theta$ polarization; (b) bistatic RCS with $\theta\phi$ polarization.

the dimensions of the square patch are 36.6 mm and 26 mm, distance between two adjacent patches is 55.517 mm in both x and y directions, the dimensions of finite substrate in x and y directions are 247.6 mm and 237 mm. The thickness for substrate is 1.58 mm. The co-polarized and cross-polarized bistatic RCS for dielectric substrate with $\chi_r = 0, \kappa_r \neq 0$ and $\chi_r \neq 0, \kappa_r \neq 0$ are calculated, as shown in Figs. 4(a) and (b). According to Figs. 4(a) and (b), we can know that the co-polarized bistatic RCS approximately remains unchanged and the cross-polarized bistatic RCS obviously increases with the growth of χ_r and κ_r.

Next, we consider the plane wave scattering from a structure consisting of conducting and dielectric objects, as shown in Fig. 5(a). The conducting bar with length of 3.5 m and width of 0.5 m and height of 0.5 m is beneath four dielectric bars. Each of dielectric bars has the same width as conducting bar and its length and height are 4 m and 2 m, respectively. The relative permittivity and permeability in this example are similar to those in the first example. MLGFIM is used to

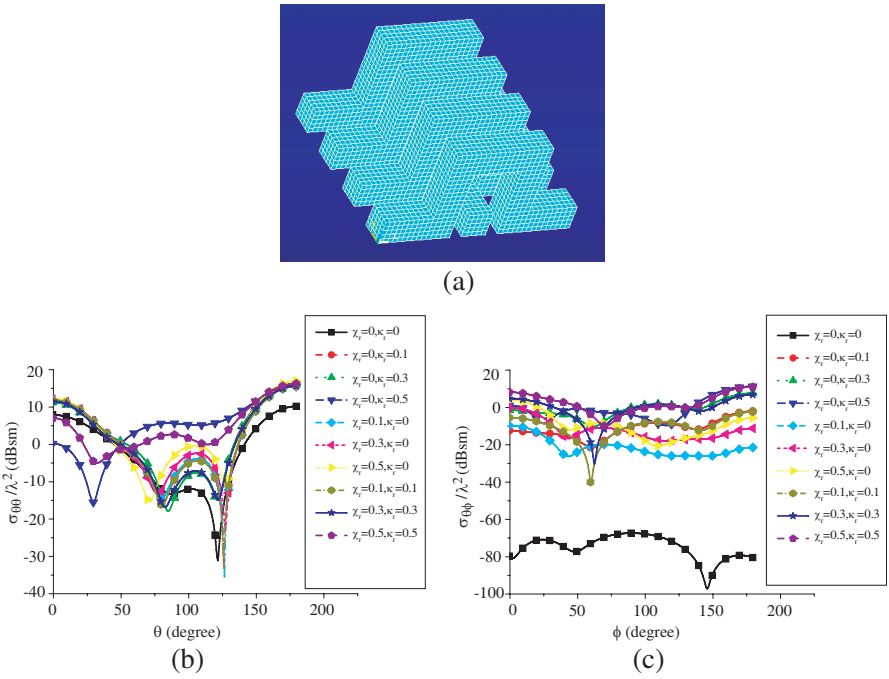

Figure 5. Plane wave scattering from a structure consisting of conducting and dielectric objects: (a) geometry, (b) bistatic RCS with $\theta\theta$ polarization; (c) bistatic RCS with $\theta\phi$ polarization.

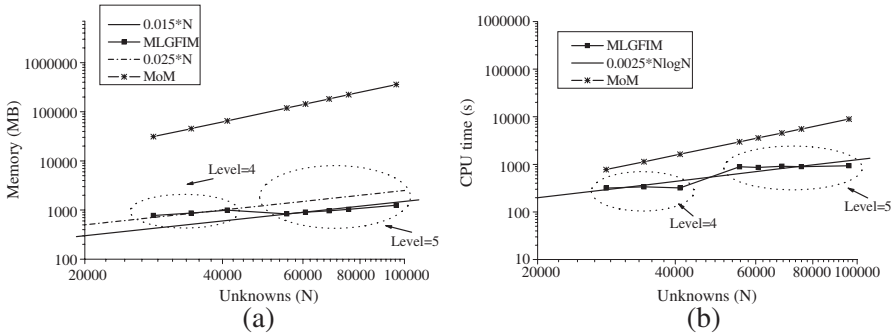

Figure 6. Computational performance of MLGFIM for bi-isotropy: (a) memory complexity, (b) computational complexity.

calculate the co-polarized and cross-polarized bistatic RCS, as shown in Figs. 5(b) and (c). According to Figs. 5(b) and (c), it can be seen that the co-polarized RCS for $\chi_r \neq 0$ or/and $\kappa_r \neq 0$ is larger than the co-polarized RCS for $\chi_r = 0, \kappa_r = 0$ in the direction of $\theta = 180°$. But the co-polarized RCS for $\kappa_r = 0.5$ is smaller than the co-polarized RCS for $\kappa_r = 0$ in the direction of $\theta = 0°$. The cross-polarized bistatic RCS for $\chi_r \neq 0$ or/and $\kappa_r \neq 0$ is larger than that for $\chi_r = 0, \kappa_r = 0$ in all directions.

Finally, we illustrate the computational performance of MLGFIM for solution to electromagnetic scattering from bi-isotropic media. Here the case of 3-by-3 sphere array with $\kappa_r = 0.5$ in first example is considered. The memory complexity and computational complexity are shown in Figs. 6(a) and (b), respectively. According to Fig. 6(a), we can know that the memory requirement for given number of levels obeys $O(N)$ and the coefficient of the line obeying $O(N)$ reduces with the increasing number of levels. It can be seen from Fig. 6(b) that computational complexity is $O(N \log N)$ and the CPU time slow increases for given number of levels.

4. CONCLUSION

In this paper, MLGFIM is proposed to solve electromagnetic scattering from arbitrary objects comprised of both conducting and bi-isotropic objects. The homogeneous bi-isotropic media are split into two uncoupled isotropic media by using the field decomposition method. The resultant problem is formulated using PMCHWT approach for homogeneous bi-isotropic objects and EFIE formulation is used for conducting bodies. MLGFIM is employed to accelerate the solution of

equivalent electromagnetic surface currents. The memory complexity of the whole algorithm is $O(N)$ and computational complexity is $O(N \log N)$. Numerical examples were presented to illustrate the accuracy and versatility of the proposed method in dealing with a wide array of scattering problems.

ACKNOWLEDGMENT

This research was supported by the National Nature Science Foundation of China No. 60801040 and No. 60601028 and the Hong Kong Research Grant Council under CERG Grant CityU110606.

REFERENCES

1. Lindell, I. V., A. H. Sihvola, S. A. Tretyakov, and A. J. Viitanen, *Electromagnetic Waves in Chiral and Bi-isotropic Media*, Artech House, Norwood, MA, 1994.
2. Serdyukov, A., I. Semchenko, S. Treyakov, and A. Sihvola, *Electromagnetics of Bi-anisotropic Materials Theory and Applications*, Gordon and Breach Science Publishers, Amsterdam, 2001.
3. Bohren, C. F., "Light scattering by an optically active sphere," *Chem. Phys. Lett.*, Vol. 29, 458–462, 1974.
4. Bohren, C. F., "Scattering of electromagnetic waves by an optically active cylinder," *J. Colloid Interface Sci.*, Vol. 66, 105–109, 1978.
5. Worasawate, D., J. R. Mautz, and E. Arvas, "Electromagnetic scattering from an arbitrarily shaped three-dimensional homogeneous chiral body," *IEEE Trans. Antennas Propagat.*, Vol. 51, 1077–1084, 2003.
6. Wang, D. X., E. K. N. Yung, R. S. Chen, and P. Y. Lau, "An efficient volume integral equation solution to EM scattering by complex bodies with inhomogeneous bi-isotropy," *IEEE Trans. Antennas Propagat.*, Vol. 55, 1970–1980, 2007.
7. Semichaevsky, A., A. Akyurtlu, D. Kem, D. H. Werner, and M. G. Bray, "Novel BI-FDTD approach for the analysis of chiral cylinders and spheres," *IEEE Trans. Antennas Propagat.*, Vol. 54, 925–932, 2006.
8. Akyurtlu, A. and D. H. Werner, "A novel dispersive FDTD formulation for modeling transient propagation in chiral metamaterials," *IEEE Trans. Antennas Propagat.*, Vol. 52, 2267–2276, 2004.
9. Sharma, R. and N. Balakrishnan, "Scattering of electromagnetic

waves from arbitrary shaped bodies coated with a chiral material," *Smart Mater. Struct.*, Vol. 7, 851–866, 1998.

10. Sheng, X. Q., J. M. Jin, J. M. Song, W. C. Chew, and C. C. Lu, "Solution of combined-field integral equation using multilevel fast multipole algorithm for scattering by homogeneous bodies," *IEEE Trans. Antennas Propagat.*, Vol. 46, 1718–1726, 1998.
11. Kolundzija, B. M., "Electromagnetic modeling of composite metallic and dielectric structures," *IEEE Trans. Microw. Theory Tech.*, Vol. 47, 1021–1032, 1999.
12. Donepudi, K. C., J. M. Jin, and W. C. Chew, "A higher order multilevel fast multipole algorithm for scattering from mixed conducting/dielectric bodies," *IEEE Trans. Antennas Propagat.*, Vol. 51, 2814–2821, 2003.
13. Yla-Oijala, P., M. Taskinen, and J. Sarvas, "Surface integral equation method for general composite metallic and dielectric structures with junctions," *Progress In Electromagnetic Research*, PIER 52, 81–108, 2005.
14. Wang, H. G., C. H. Chan, and L. Tsang, "A new multilevel Green's function interpolation method for large-scale low-frequency EM simulations," *IEEE Trans. Comput. Aided Des. Integr. Circuits Syst.*, Vol. 24, 1427–1443, 2005.
15. Wang, H. G. and C. H. Chan, "The implementation of multilevel Green's function interpolation method for full-wave electromagnetic problems," *IEEE Trans. Antennas Propagat.*, Vol. 55, 1348–1358, 2007.
16. Li, L., H. G. Wang, and C. H. Chan, "An improved multilevel Green's function interpolation method with adaptive phase compensation for large-scale full-wave EM simulation," *IEEE Trans. Antennas Propagat.*, Vol. 56, 1381–1393, 2008.
17. Shi, Y., H. G. Wang, L. Li, and C. H. Chan, "Multilevel Green's function interpolation method for scattering from composite metallic and dielectric objects," *J. Opt. Soc. Am. A*, Vol. 25, 2535–2548, 2008.
18. Lu, C. C. and W. C. Chew, "A multilevel algorithm for solving a boundary integral equation of wave scattering," *Microw. Opt. Tech. Lett.*, Vol. 7, 456–461, 1994.
19. Song, J. M., C. C. Lu, and W. C. Chew, "Multilevel fast multipole algorithm for electromagnetic scattering by large complex objects," *IEEE Trans. Antennas Propagat.*, Vol. 45, 1488–1493, 1997.
20. Chew, W. C., J. M. Jin, E. Michielssen, and J. M. Song, *Fast and*

Efficient Algorithms in Computational Electromagnetics, Artech House, Norwood, MA, 2001.

21. Zhao, X. W., X.-J. Dang, Y. Zhang, and C.-H. Liang, "MLFMA analysis of waveguiude arrays with narrow-wall slots," *Journal of Electromagnetic Waves and Applications*, Vol. 21, No. 8, 1063–1078, 2007.
22. Wang, P., Y.-J. Xie, and R. Yang, "Novel pre-corrected multilevel fast multipole algorithm for electrical large radiation problem," *Journal of Electromagnetic Waves and Applications*, Vol. 21, No. 13, 1733–1743, 2007.
23. Ouyang, J., F. Yang, S. W. Yang, and Z. P. Nie, "Exact simulation method VSWIE+MLFMA for analysis radiation pattern of probe-feed conformal microstrip antennas and the application of synthesis radiation pattern of conformal array mounted on finite-length PEC circular with DES," *Journal of Electromagnetic Waves and Applications*, Vol. 21, No. 14, 1995–2008, 2007.
24. Phillips, J. R. and J. K. White, "A precorrected-FFT method for electrostatic analysis of complicated 3-D structures," *IEEE Trans. Comput. Aided Des. Integr. Circuits Syst.*, Vol. 16, 1059–1072, 1997.
25. Nie, X. C., N. Yuan, L. W. Li, Y. B. Gan, and T. S. Yeo, "A fast volume-surface integral equation solver for scattering from composite conducting-dielectric objects," *IEEE Trans. Antennas Propagat.*, Vol. 52, 818–824, 2005.
26. Yuan, T., L.-W. Li, M.-S. Leong, J.-Y. Li, and N. Yuan, "Efficient analysis and design of finite phased arrays of printed dipoles using fast algorithm: Some case studies," *Journal of Electromagnetic Waves and Applications*, Vol. 21, No. 6, 737–754, 2007.
27. Mittra, R., *Computer Techniques for Electromagnetics*, Permagon, Elmsford, NY, 1973.
28. Mautz, J. R. and R. F. Harrington, "Electromagnetic scattering from a homogeneous material body of revolution," *AEU*, Vol. 33, 71–80, 1979.
29. Graglia, R. D., D. R. Wilton, and A. F. Peterson, "Higher order interpolatory vector bases for computational electromagnetics," *IEEE Trans. Antennas Propagat.*, Vol. 45, 329–342, 1997.
30. Horn, R. A. and C. R. Johnson, *Topics in Matrix Analysis*, Cambridge University Press, New York, 1991.
31. Wang, H. G., C. H. Chan, L. Tsang, and K. F. Chan, "Mixture effective permittivity simulations using IMLMQRF method on preconditioned EFIE," *Progress In Electromagnetics Research*,

PIER 57, 285–310, 2006.

32. Saad, Y. and M. Schultz, "GMRES: A generalized minimal residual algorithm for solving non symmetric linear systems," *SIAM J. Sci. Stat. Comput.*, Vol. 7, 856–869, 1986.
33. Rui, P.-L. and R.-S. Chen, "Implicitly restarted gmres fast fourier transform method for electromagnetic scattering," *Journal of Electromagnetic Waves and Applications*, Vol. 21, No. 7, 973–986, 2007.
34. King, A. S. and W. J. Bow, "Scattering from a finite array of microstrip patches," *IEEE Trans. Antennas Propagat.*, Vol. 40, 770–774, 1992.